

## SOLAR ENERGY CONTROL AND POWER QUALITY IMPROVEMENT USING MULTILAYER FEED FORWARD NEURAL NETWORK

R. Dehini<sup>1,\*</sup>, B. Berbaoui<sup>2</sup>

### ABSTRACT

Oil, coal and gas continue to be the most demanded source of energy throughout the world along. In recent years, the alarming fall in amounts of fossil fuels and increase in atmospheric carbon dioxide composition have been seen on several occasions. These disadvantages of fossil fuels orientate the researchers toward renewable energy sources as a more durable long-term solution. The aim of this paper is to present a shunt active power filter (PAPF) supplied by the Photovoltaic cells, in such a way that the (PAPF) feeds the linear and nonlinear loads by harmonics currents and the excess of the energy is injected into the power system. In order to improve the performances of conventional (PAPF) This paper also proposes artificial neural networks (ANN) for harmonics identification and DC link voltage control. The simulation study results of the new (SAPF) identification technique are found quite satisfactory by assuring good filtering characteristics and high system stability.

**Keywords:** *Harmonics Current, MLFFN, Photovoltaic Cells, MPPT, Shunt Active Power Filter SAPF*

### INTRODUCTION

The system of Photovoltaic power generation is a principal efficient technique of using solar energy, which can convert sunlight radiation directly into electricity through the photovoltaic effect, and has broad prospects for development with a series of advantages such as clean and pollution-free, noise-free, and renewable [1-2].

Non-linear devices produce distorted current waveforms in the power system. The injected harmonics have several impacts on the utilities grid and loads connected to system. To overcome these power quality problems, harmonic active filters are widely used in the system. [3-8]. In this paper, the analysis are focused on the system configuration with a direct coupling between the Photovoltaic cells and the shunt active power filter employed to inject the solar power into the utility grid under fixed Photovoltaic power conditions. The proposed design is not only able of delivering the solar power to the grid, but will also act as a parallel active power filter (PAPF) to mitigate the current harmonics and regulate reactive power injected by the non-linear loads. In order to investigate and mitigate the harmonic capabilities of the proposed system; a 1MW Photovoltaic power with shunt active power filter connected to a three-phase power grid feeding non-linear load was simulated in MATLAB / SIMULINK environment.

Parallel active power filter is a power converter utilized in order to compensate current disturbances (harmonics, reactive power and unbalance). In order to meet quality enhancement constraints proper control of its power switches is needed. Several topologies and configuration have been introduced in the literature and in commercial implementations for this filter that highlight different aspects of its compensation tasks. The most common topology of the shunt active power filter is shown in fig. 1. Its main components are voltage source inverter, DC bus (in our situation is a capacitor), output passive filter and a control system. The most important objective of the PAPF is to compensate the current harmonics generated by non linear loads. The reference currents consists of the harmonic components of the load currents which the active filter must supply [9]. These reference currents are fed through a controller to generate switching signals for the power switching devices of the voltage source inverter (VSI). Finally, the AC supply will only need to provide the fundamental component for the non linear load.

*This paper was recommended for publication in revised form by Regional Editor Balaram Kundu*

<sup>1</sup>University Tahri Mohamed of Bechar BP 417, Algeria

<sup>2</sup>Unité de recherche en Energie Renouvelables en milieu saharien, URERMS, Centre de Développement des Energies Renouvelables, CDER, 01000, Adrar, Algeria

\*E-mail address: [dehini\\_ra@yahoo.fr](mailto:dehini_ra@yahoo.fr)

Manuscript Received 28 May 2017, Accepted 1 October 2017

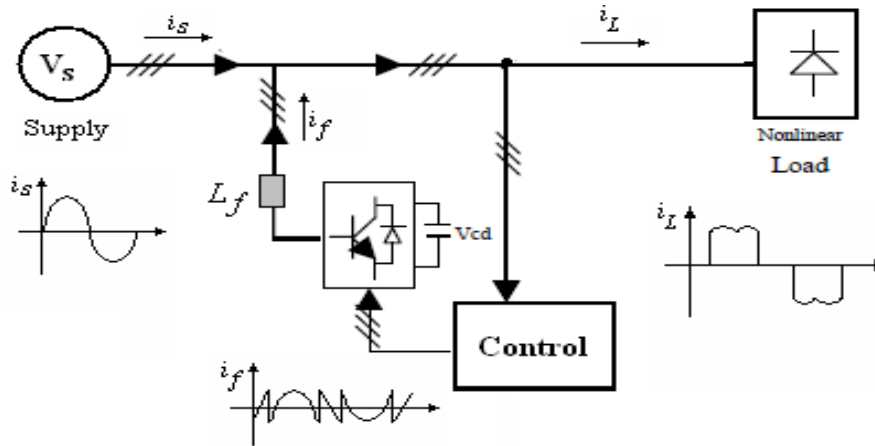


Figure 1. General structure of parallel active power filter

**PHOTOVOLTAIC GENERATOR MODELING**

Electrical energy needs are still increasing over these last years but production constraints like pollution [10] and global warming lead to development of renewable energy sources, particularly photovoltaic energy. Due to very limited conversion efficiency, it is necessary to optimize all the conversion chain and specifically DC-DC converters by use to maximum power point tracking strategies (Figure 2).

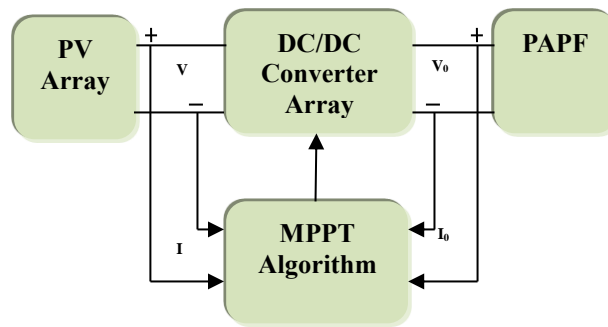


Figure 2. Block diagram of typical MPPT system

Photovoltaic generators consist usually of several modules interconnected in series and parallel for a given operating voltage an output power. Photovoltaic generators modeling can then be deduced from those of solar cells; many studies have been already proposed using one diode or more precise two diodes models. In this paper we use the conventional single diode model presented on Figure 3.

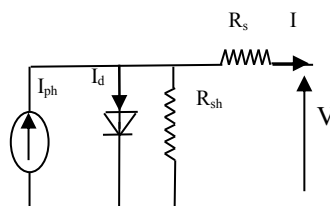


Figure 3. Conventional single diode model.

$I_{ph}$  is the photo generated current related to the illumination level,  $I_d$  the diode current,  $R_{sh}$  and  $R_s$  are respectively the shunt and series resistances. Based on Figure 3, the output voltage and current dependence can be written in the form:

$$I = I_{ph} - I_0 \left( e^{\frac{V+R_s I}{V_t}} - 1 \right) - \frac{V+R_s I}{R_{sh}} \tag{1}$$

$V_t$  is the thermal voltage written as:  $V_t = (A \cdot K \cdot T - 1)/q$  where  $A$  is the ideality factor,  $K$  the Boltzmann constant,  $T$  the temperature of the cell and  $q$  the elementary charge.

$I_0$  is the dark current. Compared to the measured photocurrent  $I_{ph\_ref}$  at standard tests conditions (STC:  $G_{ref} = 1000W/m^2$ ,  $T_{ref} = 25^\circ C$ ), the photocurrent at another operating conditions can be expressed as:

$$I_{ph} = \frac{G}{G_{ref}} [I_{ph\_ref} + \alpha(T - T_{ref})] \quad (2)$$

$G$  is the solar irradiance,  $\alpha$  is the short circuit current temperature coefficient.  $I_{ph\_ref}$  can be taken to be the short current at STC ( $I_{cc\_ref}$ ),  $I_{sc\_ref}$  and  $\alpha$  are generally given by solar module manufacturer. In the case where the cell temperature  $T_{amb}$  not is determined directly by a temperature sensor, it can be deduced from the following relation:

$$T = T_{amb} + \left[ \frac{N_{oct} - 20}{800} \right] \quad (3)$$

$T_{amb}$  is the ambient temperature,  $N_{oct}$  is the normal operating cell temperature given in most cases by the manufacturer. For the dark current  $I_0$  and we can write:

$$I_0 = I_{0\_ref} \left( \frac{T}{T_{ref}} \right)^{3/A} \exp \left[ \frac{qE_g}{AK} \left( \frac{1}{T_{ref}} - \frac{1}{T} \right) \right] \quad (4)$$

$I_{0\_ref}$  is the dark current at STC and  $E_g$  is the forbidden band energy. In the single diode model, we assumed  $R_{sh}$  to be infinite; the series resistance can be derived in the form [6]:

$$R_s = - \frac{dV}{dI(VOC)} - \frac{AKT/q}{I_0 \exp \left[ \frac{qV_{oc}}{AKT} \right]} \quad (5)$$

Equation (1) can be solved by numerical method like Newton Raphsons.

$$X_{n+1} = X_n - \frac{f(X_n)}{f'(X_n)} \quad (6)$$

The VSI is controlled in such a way that it can be used to inject sinusoidal current into the grid for energy extraction from the Photovoltaic cells during linear or non-linear load conditions. During non-linear load conditions, VSI can be used also as PAPF for harmonic and reactive compensation. To control the performance and the effectiveness of the Photovoltaic cells, the VSI is operated based on the concept of p-q theory. The control input is a current error signal which in this application, is the difference between the actual current injected by VSI and the desired or reference current waveform.

## NEURAL NETWORKS FOR REFERENCE SOURCE CURRENT AND DC VOLTAGE CONTROL

Nowadays, one of the most popular topologies in use is The MLFFN Multilayer Feed Forward Neural Network [11-12]. This network consists of a set of output neurons and one or more of intermediate neurons, known as hidden layers. Firstly, the piece of information feeds through the network by the input layer, passes across the hidden layers and finally moves out via the output layer. A three layer MLFFN interconnected by weight matrices  $W$  and bias vectors  $b$  which are the free parameters, the block diagram is illustrated by the “Fig. 4” and “Fig. 5”.

In order to modify  $W$  and  $b$ , the ANN uses the training, in such a way that the ANN approximates there function to the system function, the ANN minimizes the difference between the actual output  $y$  and the reference function. Each input in the input column vector  $x$  is weighted with an appropriate  $W$ . The sum of the weighted inputs and the bias forms the input to the transfer function  $f$ .

The activation vector “a” is determined as:

$$a = \sum(w \cdot x + b) \tag{7}$$

Neurons can use any differentiable transfer function  $f$  to generate their output. In this case the tan-sigmoid transfer function  $tansig$  function is used in input layer and the hidden layer.

$$tansig(a) = \frac{2}{1+e^{-2a}} - 1 \tag{8}$$

On the other hand the output layer uses the linear transfer function  $purelin$ .

$$Purelin(a) = a \tag{9}$$

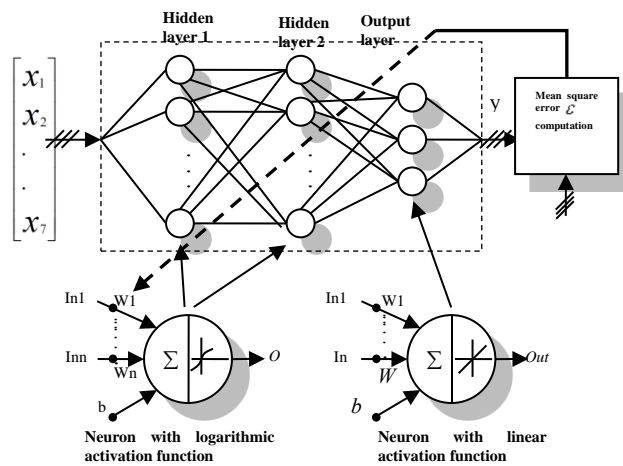


Figure 4. Neural network for (controller method) modeling

In this work the least mean square error (LMS) algorithm is used to supervise training, in which the learning rule is provided with a set of desired network behavior:

$$\{x_1, y_1\}, \{x_2, y_2\}, \dots \dots \{x_n, y_n\} \tag{10}$$

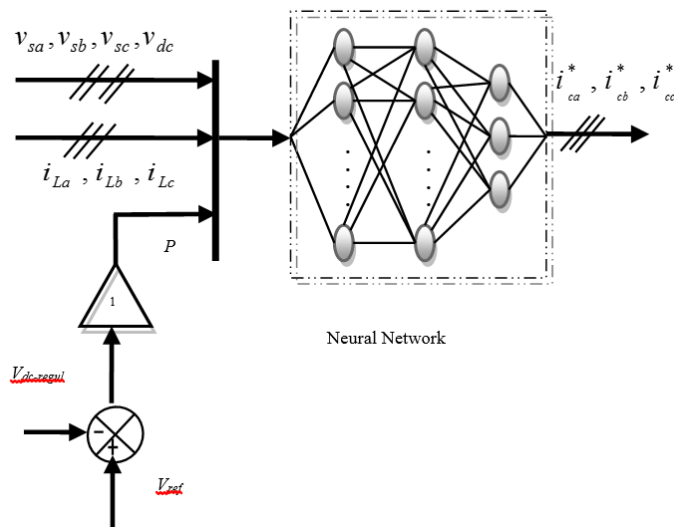


Figure 5. Controller test system model of. (Adaptive ANN)

Here is an input to the network, and is the corresponding target output. As each input is applied to the network, the network output is compared to the target. The error is calculated as the difference between the target output and the network output. The mean of the sum of these errors is calculated as:

$$\varepsilon = \frac{1}{n} \sum_{k=1}^n e(k)^2 \quad (11)$$

$$\varepsilon = \frac{1}{n} \sum_{k=1}^n (y(k) - \hat{y}(k))^2 \quad (12)$$

Where:  $\hat{y}(k)$  is the network output,  $y(k)$  is the target output.

The adjustment of the weight (W) and bias (b) in the ANN is based, firstly, on the calculation of the mean square error (LMS), and secondly, the performance of the algorithm "Levenberg-Marquardt backpropagation". The identification and filtering are carried out, for each phase, after removal from the electrical network, the load current is factorized into a Fourier series as follows:

$$i_c(t) = i_{lf}(t) + i_{lh}(t) \quad (13)$$

In this expression  $i_{lf}(t)$  represents the fundamental current and  $i_{lh}(t)$  represents the harmonic current as:

$$i_{lf}(t) = I_{11} \cos(\omega t - \alpha) + I_{12} \sin(\omega t - \alpha) \quad (14)$$

$$i_{lh}(t) = \sum_{n=2}^{49} I_{n1} \cos(n\omega t - \alpha) + I_{n2} \sin(n\omega t - \alpha) \quad (15)$$

Where  $\omega$  is the fundamental frequency of the electricity network,  $\alpha$  is an arbitrary angle which may be equal to zero,  $I_{11}$  and  $I_{12}$  are the amplitudes associated with the cosine and sine of the fundamental current,  $I_{n1}$  and  $I_{n2}$  are associated with the cosine and sine harmonic current.

The outputs of this network ( $i_{ca}^*$ ,  $i_{cb}^*$ ,  $i_{cc}^*$ ) are three terms cosine and sine from the Fourier series decomposition.

$$i_{ca}^* = i_f(t) + \sum_{n=2}^{49} I_{n1} \cos(n\omega t - \alpha) + I_{n2} \sin(n\omega t - \alpha) \quad (16)$$

Where:  $i_f(t)$  : represents the fundamental current for charging the capacitor.

## SIMULATION RESULTS AND DISCUSSION

The proposed Photovoltaic cells are not only capable of supplying extracted solar power to the power system, but it also can significantly mitigate harmonic currents which are drawn by non-linear loads. In order to demonstrate the validity of the concepts discussed previously a simulation using MATLAB/SIMULINK environment is done as it is shown in Figure 6. The parameters of the system are shown in table I.

The simulation results of the proposed PAF with PV are shown in the Figure 6. PV cells produces less than 600W at 600 Volts, so cells are connected in series and parallel to produce enough power. At 0.2 second the photovoltaic power is increasing what makes the absorbed current from the source by the non linear load decreases. At approximately 0.6 second the photovoltaic cells produces 3% of the power needed by the non linear load and the current of the source decreases to 162.1 A (RMS), the current supply decrease (Figure 7) means that the active power is injected by PAF to release the excess power in the DC bus condenser, so as to stabilize its voltage (Figure 9). We can say that the photovoltaic cells starts delivering power to the grid after it has finished feeding the PAF by all the power it needs. Finally, it is clear that the PAF injects appropriate amount of current to mitigate harmonics generated by the non linear load and at the same time deliver the excess active power to the grid.

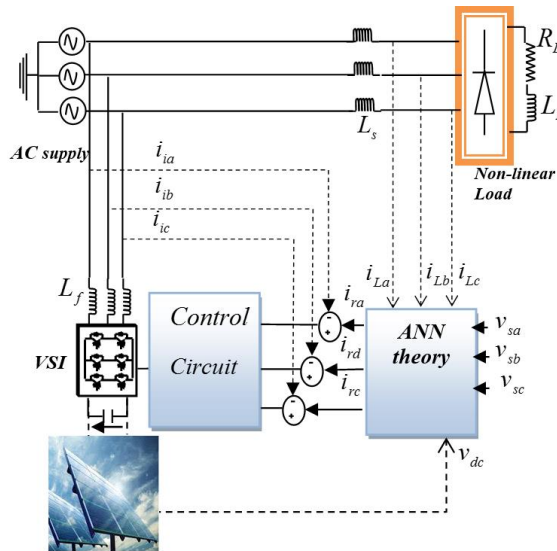
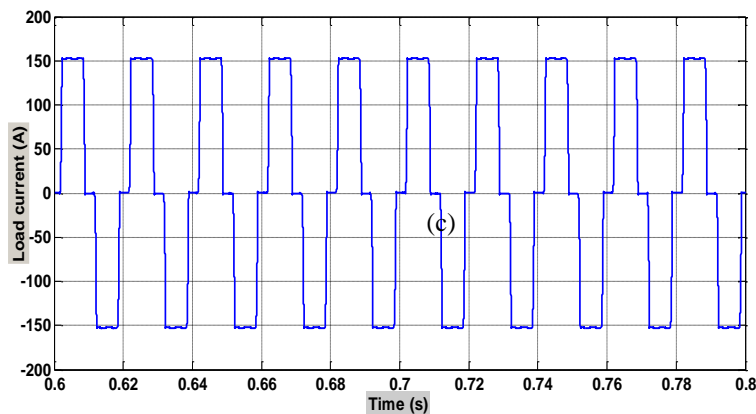


Figure 6. SIMULINK Implementation of PAPF with PV

The ANN in “Fig. 3” has seven inputs ( $v_{sa}, v_{sb}, v_{sc}, P_f, i_{sa}, i_{sb}, i_{sc}$ ) and three outputs ( $i_{ca}^*, i_{cb}^*, i_{cc}^*$ ). This ANN is made up of two hidden layers, each layer contains 12 neurons, and an output layer with 3 neurons. The hyperbolic tangent sigmoid activation function is used for the two hidden layers and a linear activation function for the output layer neurons.

Table 1. System parameters

Grid	
Source Voltage $V_s$	220 V
Load Power $P_L$	80 kVA
Frequency $f_s$	50 Hz
Photovoltaic cells	
Nominal Power $P_T$	24 KW
cells Voltage $V_T$	850 V
PAPF	
Switching Frequency	12 kHz
Output Filter	1 mH
DC Link Capacitor	8.8 mF
Capacitor DC Voltage	2600 V
reference current	p-q Method
VSI control	PWM + PI



(a)

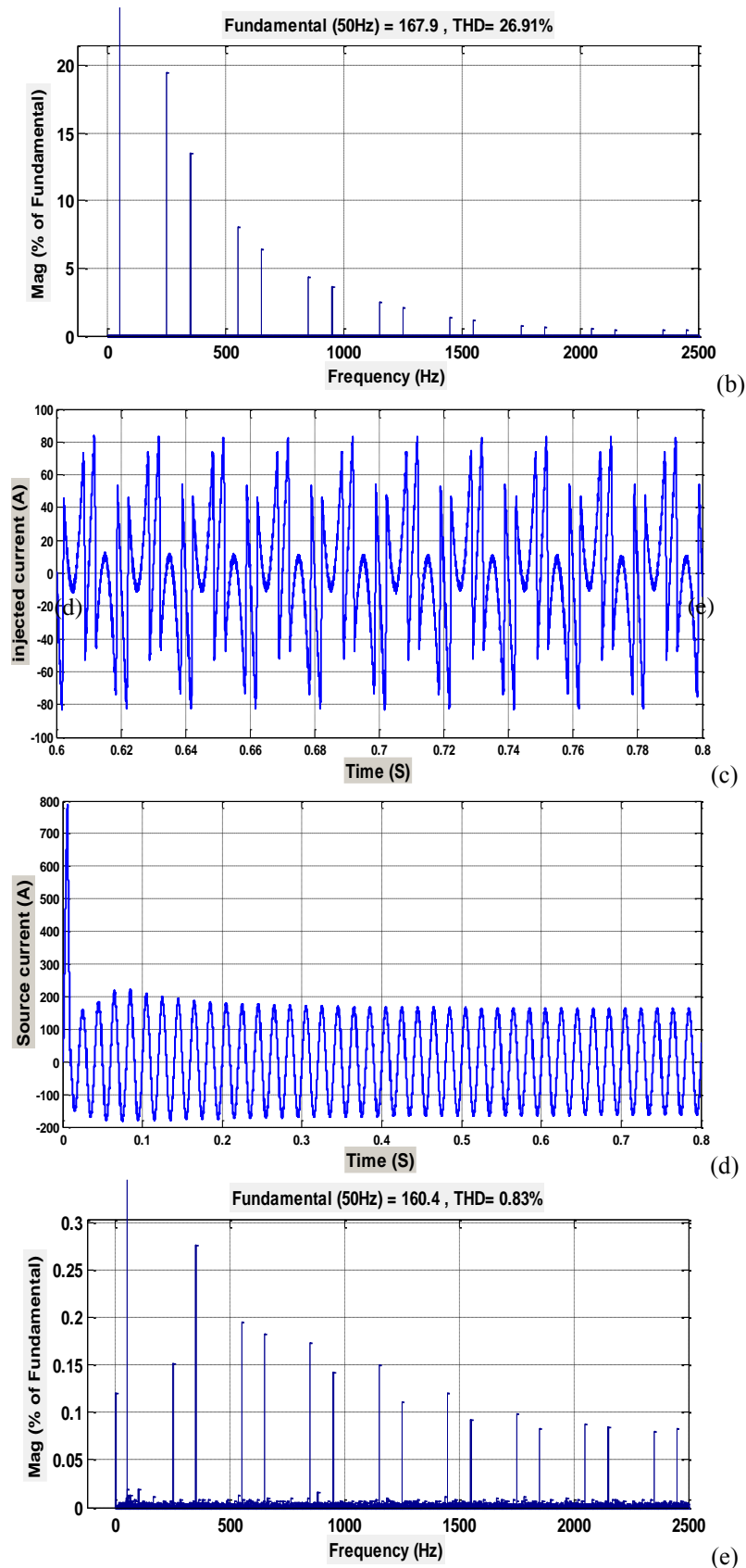


Figure 7. (a) phase-a load current, (b) Harmonic spectrum of load current Phase 'a', (c) phase-a reference current, (d) phase-a the supply current, (e) Harmonic spectrum of supply current Phase 'a', with (PV).

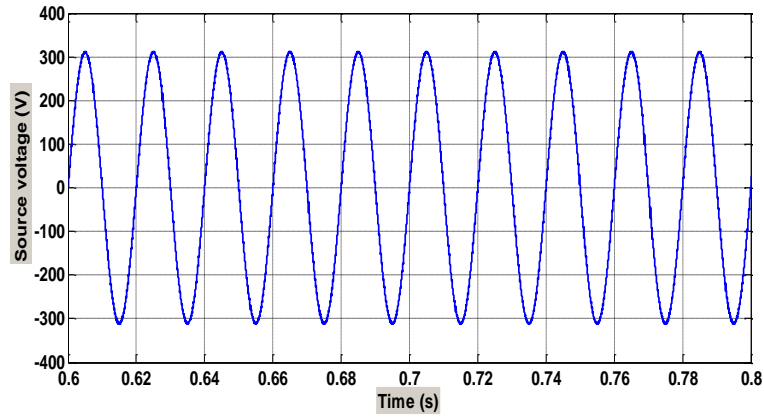


Figure 8. Phase-a the supply voltage waveforms, with a (PV).

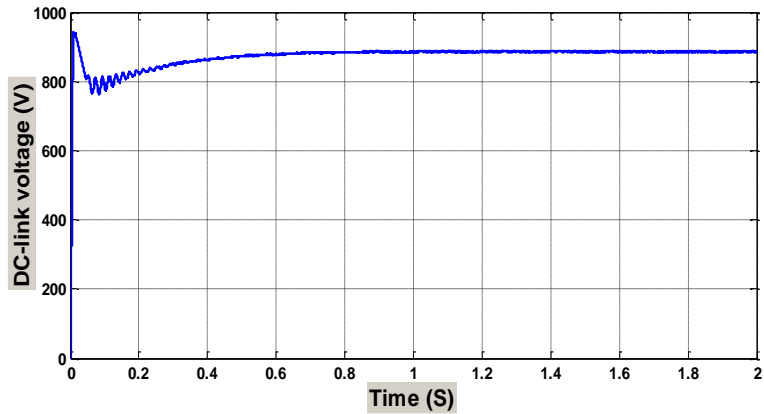


Figure 9. DC-link voltage.

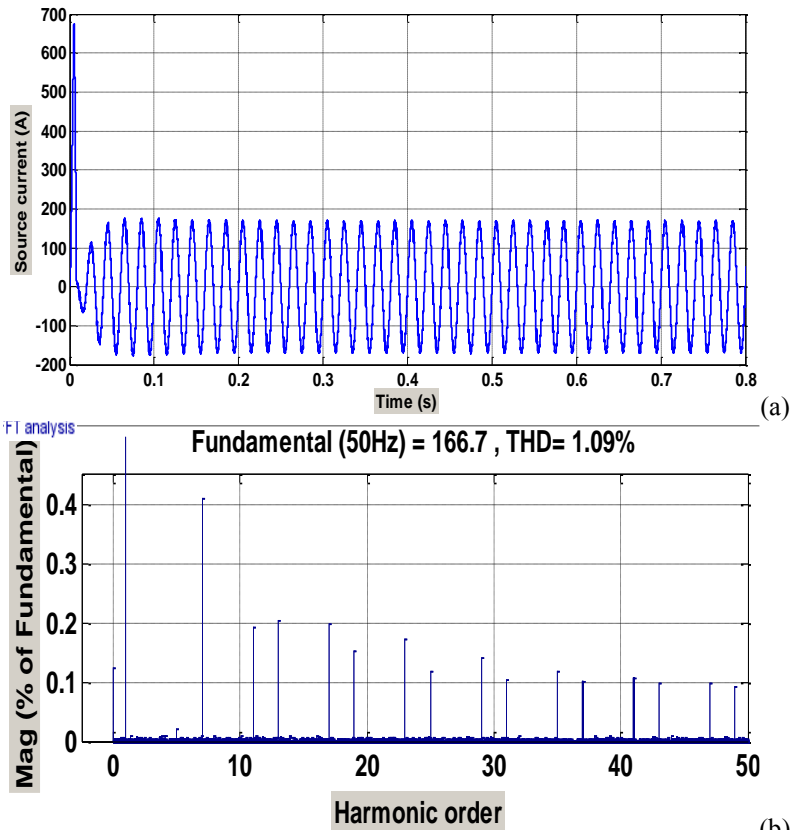


Figure 10. (a) phase-a the supply current, (b) Harmonic spectrum of supply current Phase 'a', without a (PV).



## CONCLUSION

In order to optimize the use of Photovoltaic power this work has proposed a direct association between the Photovoltaic cells and parallel active power filters (PAPF). The later possessed two functions; the first is feeding the linear or non linear load with harmonic current mitigation capability and second injecting the surplus power into the power system. The (PAPF) use a new method of power control and detection based on artificial neural network (ANN). The obtained results prove that the proposed system is the efficient solution to the growing demand of power at the present and in the future.

## REFERENCES

- [1] Busa, V., Narsingoju, K. K., & Kumar, G. V. (2012). Simulation analysis of maximum power control of photo voltaic power system. *International Journal on Advanced Electrical and Electronics Engineering (IJAEED)*, 1(1), 9-14.
- [2] Setiawan, E. A., Setiawan, A., & Siregar, D. (2017). Analysis on solar panel performance and pv-inverter configuration for tropical region. *Journal of Thermal Engineering*, 3(3), 1259-1270.
- [3] Jeong, G. Y., Park, T. J., & Kwon, B. H. (2000). Line-voltage-sensorless active power filter for reactive power compensation. *IEE Proceedings-Electric Power Applications*, 147(5), 385-390.
- [4] Izhar, M., Hadzer, C. M., Syafrudin, M., Taib, S., & Idris, S. (2004). Performance for passive and active power filter in reducing harmonics in the distribution system. In *Power and Energy Conference, 2004. PECon 2004 Proceedings*, 104-108.
- [5] Gao, D., Lu, Q., & Sun, X. (2002). Design and performance of an active power filter for unbalanced loads. In *Power System Technology, 2002. ProceedingsmPowerCon 2002*, 2496-2500.
- [6] Tumbelaka, H. H. (2006). A grid current-controlling shunt active power filter using polarized ramp-time current control. Curtin University of Technology.
- [7] Tumbelaka, H. H., Borle, L. J., & Nayar, C. V. (2002). Application of a shunt active power filter to compensate multiple non-linear loads. In *Australasian Universities Power Engineering Conference (AUPEC)*.
- [8] Tumbelaka, H. H., Nayar, C. V., Tan, K., & Borle, L. J. (2003). Active filtering applied to a line-commutated inverter fed permanent magnet wind generator. In *International Power Engineering Conference IPEC2003, Singapore*.
- [9] Wada, K., Fujita, H., & Akagi, H. (2002). Considerations of a shunt active filter based on voltage detection for installation on a long distribution feeder. *IEEE Transactions on Industry Applications*, 38(4), 1123-1130.
- [10] Yahfdhou, A., Mahmoud, A., & Youm, I. (2013). Modeling and optimization of a photovoltaic generator with matlab/simulink. *International Journal of I Tech and E Engineering*, 3(4), 108-111.
- [11] Dehini, R., Bassou, A., & Ferdi, B. (2009). Artificial neural networks application to improve shunt active power filter. *International Journal of Computer and Information Engineering*, 3(4), 247-254.
- [12] Pusat, S., & Akkoyunlu. (2018). Effect of time horizon on wind speed prediction with ANN. *Journal of Thermal Engineering*, 4 (2), pp. 1770-1779.